PNAS
www.pnas.org

Supplementary Information for

Dynamic population stage-structure due to juvenile-adult asymmetry stabilises complex ecological communities

André M. de Roos

Corresponding Author: André M. de Roos.
E-mail: A.M.deRoos@uva.nl

This PDF file includes:

Supplementary text
Figs. S1 to S10 (not allowed for Brief Reports)
SI References

Supporting Information Text

Model reformulation and analysis

The stage-structured model in terms of the juvenile and adult densities J_i and A_i, respectively, can be reformulated into a model in terms of the total number of individuals of species i and the fraction of juveniles in the population of species i. Define C_i as the total density, $C_i = J_i + A_i$, and Z_i as the fraction of juveniles of species i, $Z_i = J_i/C_i$. Using these alternative model variables the functional response value for the basal species can be written as:

$$F_1 = \frac{P}{\delta + \alpha_1 \left(qZ_1 + (2-q)(1-Z_1)\right) C_1} \quad [1]$$

and the encounter rate of all non-basal species with their prey as

$$E_i = \sum_{k<i} \psi_{ik} \left(\phi Z_k + (2-\phi)(1-Z_k)\right) C_k \quad [2]$$

From the ordinary differential equations (ODEs) for the juvenile and adult densities J_i and A_i presented in the Materials and Methods section, the following system of ODEs for the alternative model variables C_i and Z_i can then be derived through analytical manipulation:

$$\begin{aligned}\frac{dC_i}{dt} &= b_i(F_i)(1-Z_i)C_i - \mu_i C_i \\ &\quad - \left(\phi Z_i + (2-\phi)(1-Z_i)\right) C_i \sum_{k>i} \alpha_k \psi_{ki} \frac{\left(qZ_k + (2-q)(1-Z_k)\right) C_k}{H_k + E_k}\end{aligned} \quad [3]$$

$$\begin{aligned}\frac{dZ_i}{dt} &= b_i(F_i)(1-Z_i)^2 - m_i(F_i)Z_i \\ &\quad -2(\phi-1)(1-Z_i)Z_i \sum_{k>i} \alpha_k \psi_{ki} \frac{\left(qZ_k + (2-q)(1-Z_k)\right) C_k}{H_k + E_k}\end{aligned} \quad [4]$$

Model simplification in case of ontogenetic symmetry. Assuming ontogenetic symmetry in ingestion and per-capita predation risk between juveniles and adults is equivalent to setting both q and ϕ equal to 1, which simplifies the per-capita reproduction and maturation rate to:

$$b_i(F_i) = m_i(F_i) = \max\left(\gamma_i F_i - T_i, 0\right)$$

while the expressions for the encounter rate of non-basal species with their prey, E_i, equals:

$$E_i = \sum_{k<i} \psi_{ik} C_k \quad [5]$$

The functional response for species i is hence given by:

$$F_i = \begin{cases} \dfrac{P}{\delta + \alpha_1 C_1} & i = 1 \\ \dfrac{\sum_{k<i} \psi_{ik} C_k}{H_i + \sum_{k<i} \psi_{ik} C_k} & \text{otherwise} \end{cases} \quad [6]$$

The equations describing the dynamics of total species densities C_i and fractions of juveniles Z_i therefore simplify to:

$$\frac{dC_i}{dt} = \max\left(\gamma_i F_i - T_i, 0\right)(1-Z_i)C_i - \mu_i C_i - \sum_{k>i} \alpha_k \psi_{ki} \frac{C_k}{H_k + E_k} C_i \quad [7]$$

$$\frac{dZ_i}{dt} = \max\left(\gamma_i F_i - T_i, 0\right)\left(1 - 3Z_i + Z_i^2\right) \quad [8]$$

For all populations (basal and non-basal) the dynamics of the fraction of juveniles Z_i hence follows a separable function, consisting of a factor $\max\left(\gamma_i F_i - T_i, 0\right)$ that only depends on the total species densities C_i and a factor $\left(1 - 3Z_i + Z_i^2\right)$ that only depends on the fraction of juveniles Z_i. Irrespective of the fluctuations in the total species densities C_i, the fraction of juveniles in each population will therefore approach the unique root in the interval [0,1] of the quadratic condition $\left(1 - 3Z_i + Z_i^2\right) = 0$ for $t \to \infty$, i.e. approach the constant value:

$$\overline{Z} = \frac{3}{2} - \frac{1}{2}\sqrt{5} \approx 0.38 \quad [9]$$

In the long run the dynamics of this juvenile-adult abundance model are therefore captured by a model that only considers total species abundances:

$$\frac{dC_i}{dt} = \max\left(\gamma_i F_i - T_i, 0\right)(1-\overline{Z})C_i - \mu_i C_i - \sum_{k>i} \alpha_k \psi_{ki} \frac{C_k}{H_k + E_k} C_i \quad [10]$$

with E_i and F_i given by Eq. (5) and Eq. (6), respectively.

Computing eigenvalues of the stage-structured model. To verify the local stability of the community states that appear to be stable based on numerical simulations I compute the eigenvalues characterising the dynamics in the neighbourhood of the equilibrium using the Jacobian matrix. In the neighbourhood of an equilibrium of the stage-structured model persistence of a species in the community guarantees that starvation does not occur for the juveniles nor the adults. In such a close neighbourhood of an equilibrium state the reproduction and maturation rate of adult and juvenile consumers are therefore necessarily positive, such that

$$b_i(F_i) = \max\left((2-q)\gamma_i F_i - T_i, 0\right) = (2-q)\gamma_i F_i - T_i \quad [11]$$

$$m_i(F_i) = \max\left(q\gamma_i F_i - T_i, 0\right) = q\gamma_i F_i - T_i \quad [12]$$

The dynamics of the total species densities C_i and the fraction of juveniles in the populations Z_i can then be described by simplified versions of the ODEs. (3) and (4):

$$\begin{aligned}\frac{dC_i}{dt} &= \left((2-q)\gamma_i F_i - T_i\right)(1-Z_i)C_i - \mu_i C_i \\ &\quad - \left(\phi Z_i + (2-\phi)(1-Z_i)\right) C_i \sum_{k>i} \alpha_k \psi_{ki} \frac{\left(qZ_k + (2-q)(1-Z_k)\right) C_k}{H_k + E_k}\end{aligned} \quad [13]$$

$$\begin{aligned}\frac{dZ_i}{dt} &= \left((2-q)\gamma_i F_i - T_i\right)(1-Z_i)^2 - \left(q\gamma_i F_i - T_i\right) Z_i \\ &\quad -2(\phi-1)(1-Z_i)Z_i \sum_{k>i} \alpha_k \psi_{ki} \frac{\left(qZ_k + (2-q)(1-Z_k)\right) C_k}{H_k + E_k}\end{aligned} \quad [14]$$

The whole system of differential equations can be summarised as:

$$\frac{d\mathbf{C}}{dt} = \mathbf{K}\left(\mathbf{C}, \mathbf{Z}\right) \quad [15]$$

$$\frac{d\mathbf{Z}}{dt} = \mathbf{L}\left(\mathbf{C}, \mathbf{Z}\right) \quad [16]$$

in which $\mathbf{C}$ and $\mathbf{Z}$ are the vectors of total species abundances and fractions of juveniles in all populations, respectively. The vector-valued functions $\mathbf{K}(\mathbf{C}, \mathbf{Z})$ and $\mathbf{L}(\mathbf{C}, \mathbf{Z})$ contain the right-hand side of the ODEs dC_i/dt (13) and dZ_i/dt (14) for the species-density subsystem, respectively.

For a community with m species the Jacobian matrix of this model is a $2m \times 2m$ matrix $\mathbf{J}$ of the form:

$$\mathbf{J} = \begin{pmatrix} \frac{\partial \mathbf{K}}{\partial \mathbf{C}} & \frac{\partial \mathbf{K}}{\partial \mathbf{Z}} \\ \frac{\partial \mathbf{L}}{\partial \mathbf{C}} & \frac{\partial \mathbf{L}}{\partial \mathbf{Z}} \end{pmatrix} = \begin{pmatrix} \mathbf{V^1} + \mathbf{W^1} & \mathbf{V^2} + \mathbf{W^2} \\ \mathbf{V^3} + \mathbf{W^3} & \mathbf{V^4} + \mathbf{W^4} \end{pmatrix} \quad [17]$$

Each of the 4 parts of J is a $m \times m$ matrix containing the partial derivatives of the functions $\mathbf{K}(\mathbf{C}, \mathbf{Z})$ and $\mathbf{L}(\mathbf{C}, \mathbf{Z})$ with respect to the total species densities $(C_1, \ldots, C_m)$ and fractions of juveniles $(Z_1, \ldots, Z_m)$. $\mathbf{V^1}$, $\mathbf{V^2}$, $\mathbf{V^3}$ and $\mathbf{V^4}$ are 4 $m \times m$ matrices that capture the direct effects of two species in the community on each other, while $\mathbf{W^1}$, $\mathbf{W^2}$, $\mathbf{W^3}$ and $\mathbf{W^4}$ are 4 $m \times m$ matrices that capture the indirect effects between two species that operates through a third species. More specifically, indirect effects occur between species because changes in the total density C_j and the fraction of juveniles Z_j influence the encounter rate E_k of a consumer species k, which in turn affects the predation rate of species k on species i (last summation terms in ODEs above). Indirect effects hence involve interactions between a predator species k and two of its prey species with indices i and j.

The elements of the matrices $\mathbf{V^1}$, $\mathbf{V^2}$, $\mathbf{V^3}$ and $\mathbf{V^4}$ are defined as:

$$V^1_{i,j} = \frac{d}{dC_j}\left(dC_i/dt\right),\ V^2_{i,j} = \frac{d}{dZ_j}\left(dC_i/dt\right),\ V^3_{i,j} = \frac{d}{dC_j}\left(dZ_i/dt\right),\ V^4_{i,j} = \frac{d}{dZ_j}\left(dZ_i/dt\right)$$

Notice however that the derivatives with respect to C_j and Z_j in these expressions are evaluated while ignoring the indirect effects that will be captured by the matrices $\mathbf{W^1}$, $\mathbf{W^2}$, $\mathbf{W^3}$ and $\mathbf{W^4}$, that is, while treating the quantities E_k in the predation mortality terms (last summation terms in ODEs (13) and (14)) as constants.

The entries V^1_{ij} are given by:

$$V^1_{ij} = \begin{cases} \left((2-q)\gamma_1 \dfrac{\delta F_1^2}{P} - T_1\right)(1-Z_1) - \mu_1 \\ \quad -(\phi Z_1 + (2-\phi)(1-Z_1)) \displaystyle\sum_{k>1} \alpha_k \psi_{k1} \frac{(qZ_k + (2-q)(1-Z_k))\, C_k}{H_k + E_k} & i = j = 1 \\ ((2-q)\gamma_i F_i - T_i)(1-Z_i) - \mu_i \\ \quad -(\phi Z_i + (2-\phi)(1-Z_i)) \displaystyle\sum_{k>i} \alpha_k \psi_{ki} \frac{(qZ_k + (2-q)(1-Z_k))\, C_k}{H_k + E_k} & i = j \neq 1 \\ -\alpha_j \psi_{ji} \dfrac{(qZ_j + (2-q)(1-Z_j))}{H_j + E_j} (\phi Z_i + (2-\phi)(1-Z_i))\, C_i & i < j \\ (2-q)\gamma_i \dfrac{H_i}{(H_i+E_i)^2} \psi_{ij} (\phi Z_j + (2-\phi)(1-Z_j))(1-Z_i) C_i & i > j \end{cases} \quad [18]$$

In the above expressions for the matrix elements V^1_{ij} with $i > j$ I have used the identities

$$\frac{dF_i}{dC_j} = \frac{dF_i}{dE_i}\frac{dE_i}{dC_j} = \frac{H_i}{(H_i+E_i)^2}\frac{dE_i}{dC_j} = \frac{H_i}{(H_i+E_i)^2}\psi_{ij}\,(\phi Z_j + (2-\phi)(1-Z_j))$$

and

$$\begin{aligned} \frac{d(F_1 C_1)}{dC_1} &= \frac{d}{dC_1}\frac{PC_1}{\delta + \alpha_1 (qZ_1 + (2-q)(1-Z_1))\, C_1} \\ &= \frac{\delta P}{(\delta + \alpha_1 (qZ_1 + (2-q)(1-Z_1))\, C_1)^2} \\ &= \frac{\delta F_1^2}{P} \end{aligned}$$

In an equilibrium state all per-capita growth rates $(dC_i/dt)/C_i$ vanish such that the entries of the matrix $\mathbf{V^1}$ simplify to:

$$V^1_{ij} = \begin{cases} (2-q)\gamma_1 \left(\dfrac{\delta F_1}{P} - 1\right) F_1 (1-Z_1) & i = j = 1 \\ 0 & i = j \neq 1 \\ -\alpha_j \psi_{ji} \dfrac{(qZ_j + (2-q)(1-Z_j))}{H_j + E_j} (\phi Z_i + (2-\phi)(1-Z_i))\, C_i & i < j \\ (2-q)\gamma_i \dfrac{H_i}{(H_i+E_i)^2} \psi_{ij} (\phi Z_j + (2-\phi)(1-Z_j))(1-Z_i) C_i & i > j \end{cases} \quad [19]$$

The entries V^2_{ij} are given by:

$$V^2_{ij} = \begin{cases} -\left((2-q)\gamma_1 \dfrac{(\delta + \alpha_1 q C_1)\, F_1^2}{P} - T_1\right) C_1 \\ \quad -2(\phi-1) C_1 \displaystyle\sum_{k>1} \alpha_k \psi_{k1} \frac{(qZ_k + (2-q)(1-Z_k))\, C_k}{H_k + E_k} & i = j = 1 \\ -((2-q)\gamma_i F_i - T_i)\, C_i \\ \quad -2(\phi-1) C_i \displaystyle\sum_{k>i} \alpha_k \psi_{ki} \frac{(qZ_k + (2-q)(1-Z_k))\, C_k}{H_k + E_k} & i = j \neq 1 \\ -\alpha_j \psi_{ji} \dfrac{2\,(q-1)\, C_j}{H_j + E_j} (\phi Z_i + (2-\phi)(1-Z_i))\, C_i & i < j \\ (2-q)\gamma_i \dfrac{H_i}{(H_i+E_i)^2} \psi_{ij} 2\,(\phi-1)\, C_j (1-Z_i) C_i & i > j \end{cases} \quad [20]$$

To derive the expressions for the matrix elements V^2_{ij} with $i > j$ I have used the identities

$$\frac{dF_i}{dZ_j} = \frac{dF_i}{dE_i}\frac{dE_i}{dZ_j} = \frac{H_i}{(H_i+E_i)^2}\frac{dE_i}{dZ_j} = \frac{H_i}{(H_i+E_i)^2}\psi_{ij} 2\,(\phi-1)\, C_j$$

and

$$\begin{aligned}\frac{d(F_1(1-Z_1))}{dZ_1} &= \frac{d}{dZ_1}\frac{P(1-Z_1)}{\delta+\alpha_1\left(qZ_1+(2-q)(1-Z_1)\right)C_1}\\ &= -\frac{\left(\delta+\alpha_1 qC_1\right)P}{\left(\delta+\alpha_1\left(qZ_1+(2-q)(1-Z_1)\right)C_1\right)^2}\\ &= -\frac{\left(\delta+\alpha_1 qC_1\right)F_1^2}{P}\end{aligned}$$

The entries V_{ij}^3 are given by:

$$V_{ij}^3 = \begin{cases} -\gamma_1\frac{\alpha_1\left(qZ_1+(2-q)(1-Z_1)\right)F_1^2}{P}\left((2-q)(1-Z_1)^2-qZ_1\right) & i=j=1\\ 0 & i=j\neq 1\\ -\alpha_j\psi_{ji}\frac{(qZ_j+(2-q)(1-Z_j))}{H_j+E_j}2(\phi-1)(1-Z_i)Z_i & i<j\\ \gamma_i\frac{H_i}{(H_i+E_i)^2}\psi_{ij}\left(\phi Z_j+(2-\phi)(1-Z_j)\right)\left((2-q)(1-Z_i)^2-qZ_i\right) & i>j\end{cases} \quad [21]$$

To derive the expressions for the matrix elements V_{ij}^3 with $i=j=1$ I have used the identity

$$\begin{aligned}\frac{dF_1}{dC_1} &= \frac{d}{dC_1}\frac{P}{\delta+\alpha_1\left(qZ_1+(2-q)(1-Z_1)\right)C_1}\\ &= -\frac{\alpha_1\left(qZ_1+(2-q)(1-Z_1)\right)P}{\left(\delta+\alpha_1\left(qZ_1+(2-q)(1-Z_1)\right)C_1\right)^2}\\ &= -\frac{\alpha_1\left(qZ_1+(2-q)(1-Z_1)\right)F_1^2}{P}\end{aligned}$$

Finally, the entries V_{ij}^4 are given by:

$$V_{ij}^4 = \begin{cases} -\gamma_1\frac{2\alpha_1(q-1)C_1F_1^2}{P}\left((2-q)(1-Z_1)^2-qZ_1\right)\\ -2\left((2-q)\gamma_1F_1-T_1\right)(1-Z_1)-(q\gamma_1F_1-T_1)\\ -2(\phi-1)(1-2Z_1)\sum_{k>1}\alpha_k\psi_{k1}\frac{(qZ_k+(2-q)(1-Z_k))C_k}{H_k+E_k} & i=j=1\\ -2\left((2-q)\gamma_iF_i-T_i\right)(1-Z_i)-(q\gamma_iF_i-T_i)\\ -2(\phi-1)(1-2Z_i)\sum_{k>i}\alpha_k\psi_{ki}\frac{(qZ_k+(2-q)(1-Z_k))C_k}{H_k+E_k} & i=j\neq 1\\ -\alpha_j\psi_{ji}\frac{2(q-1)C_j}{H_j+E_j}2(\phi-1)(1-Z_i)Z_i & i<j\\ \gamma_i\frac{H_i\psi_{ij}2(\phi-1)C_j}{(H_i+E_i)^2}\left((2-q)(1-Z_i)^2-qZ_i\right) & i>j\end{cases} \quad [22]$$

The derivation of the expressions for the matrix elements V_{ij}^4 with $i=j=1$ is based on the identity

$$\begin{aligned}\frac{dF_1}{dZ_1} &= \frac{d}{dZ_1}\frac{P}{\delta+\alpha_1\left(qZ_1+(2-q)(1-Z_1)\right)C_1}\\ &= -\frac{2\alpha_1(q-1)C_1P}{\left(\delta+\alpha_1\left(qZ_1+(2-q)(1-Z_1)\right)C_1\right)^2}\\ &= -\frac{2\alpha_1(q-1)C_1F_1^2}{P}\end{aligned}$$

As explained above, indirect effects occur between species because changes in the total density C_j and fraction of juveniles Z_j influence the encounter rate E_k of a consumer species k, which in turn affects the predation rate of species k on species i.

These indirect effects therefore always arise because of the summation terms representing predation mortality in eqs. (13) and (14). In the predation rate of species k only the term $1/(H_k + E_k)$ depends on the total density C_j and the fraction of juveniles Z_j of species j and the derivatives of this term with respect to C_j and Z_j equal

$$-\frac{1}{(H_k + E_k)^2}\psi_{kj}\left(\phi Z_j + (2-\phi)(1-Z_j)\right)$$

and

$$-\frac{1}{(H_k + E_k)^2}\psi_{kj} 2\left(\phi - 1\right) C_j$$

respectively. The elements of the matrices $\mathbf{W^1}$, $\mathbf{W^2}$, $\mathbf{W^3}$ and $\mathbf{W^4}$ are hence defined as:

$$W^1_{i,j} = \left(\phi Z_i + (2-\phi)(1-Z_i)\right) C_i \left(\phi Z_j + (2-\phi)(1-Z_j)\right) \sum_{k>i} \alpha_k \psi_{ki}\psi_{kj} \frac{\left(qZ_k + (2-q)(1-Z_k)\right) C_k}{(H_k + E_k)^2}$$

$$W^2_{i,j} = \left(\phi Z_i + (2-\phi)(1-Z_i)\right) C_i \, 2(\phi-1) C_j \sum_{k>i} \alpha_k \psi_{ki}\psi_{kj} \frac{\left(qZ_k + (2-q)(1-Z_k)\right) C_k}{(H_k + E_k)^2}$$

$$W^3_{i,j} = 2(\phi-1)(1-Z_i) Z_i \left(\phi Z_j + (2-\phi)(1-Z_j)\right) \sum_{k>i} \alpha_k \psi_{ki}\psi_{kj} \frac{\left(qZ_k + (2-q)(1-Z_k)\right) C_k}{(H_k + E_k)^2}$$

$$W^4_{i,j} = 2(\phi-1)(1-Z_i) Z_i \, 2(\phi-1) C_j \sum_{k>i} \alpha_k \psi_{ki}\psi_{kj} \frac{\left(qZ_k + (2-q)(1-Z_k)\right) C_k}{(H_k + E_k)^2}$$

Note that i and j may be equal to each other as changes in the total density of C_i and the fraction of juveniles Z_i change the predation rate of species k on species i through a change in the functional response of species k, which effect is not captured by the matrices $\mathbf{V^1}$, $\mathbf{V^2}$, $\mathbf{V^3}$ and $\mathbf{V^4}$. Furthermore, note that all elements W^1_{ij} are positive for species that are exposed to predation and equal to 0 only for top predators. Together with the fact that $V^1_{ii} = 0$ for $i \neq 0$ this implies that the effect of species density C_i on its own rate of change dC_i/dt is 0 for top predators and positive for all non-basal species experiencing predation.

All communities resulting from the stage-structured model with asymmetry in feeding and predation between juveniles and adults ($q = 0.7$, $\phi = 1.8$) for which the minimum and maximum values of the total species density differed less than 10^{-6} from each other for all species were considered stable. All communities for which the minimum and maximum values of total species density differed more than 10^{-6} from each other for at least 1 species, were considered unstable (cycling) communities. For both stable and unstable communities the average total abundance and fraction of juveniles observed in the simulation were used as starting values to numerically solve for the equilibrium state using the package 'rootSolve' (1, 2) in R (3). For all 115 stable communities the equilibrium community state was successfully located and was numerically indistinguishable from the average densities and juvenile fractions observed in the numerical simulations. For 147 communities that were considered unstable (cycling) the numerical solution procedure also converged to an equilibrium community state with all species present, while for 238 unstable communities the numerical solution procedure did not converge to such an equilibrium state.

For all communities, for which the equilibrium state was successfully located, the Jacobian matrix J was evaluated by substituting for all species the equilibrium values for the total abundance and fraction of juveniles as well as all general and species-specific parameters into the matrices $\mathbf{V^1}$, $\mathbf{V^2}$, $\mathbf{V^3}$, $\mathbf{V^4}$, $\mathbf{W^1}$, $\mathbf{W^2}$, $\mathbf{W^3}$ and $\mathbf{W^4}$. The eigenvalues of the Jacobian matrix $\mathbf{J}$ (see Eq. (17)) were subsequently computed numerically using the routine eigen() in R (3). These calculations of the Jacobian matrix based on the analytical expressions for the matrices $\mathbf{V^1}$, $\mathbf{V^2}$, $\mathbf{V^3}$, $\mathbf{V^4}$, $\mathbf{W^1}$, $\mathbf{W^2}$, $\mathbf{W^3}$ and $\mathbf{W^4}$ were verified by also computing the Jacobian matrix numerically using central differencing methods applied to the right-hand side of the ODEs (13) and (14) for dC_i/dt and dZ_i/dt.

For both stable and unstable communities the largest real part among the eigenvalues (i.e. the real part of the dominant eigenvalue) is shown in Fig. S4. For stable communities this real part was always negative, ranging between -0.061 and $-9.8 \cdot 10^{-5}$. For unstable communities this real part was always positive, ranging between $1.3 \cdot 10^{-4}$ and 0.124.

Sources of community stability. For stable communities the effect of dynamic changes in population stage-structure (i.e. changes in the juvenile-adult ratio) on the stability of the community equilibrium was evaluated further. The dominant eigenvalues computed for these communities were compared with the eigenvalues of the top-left submatrix of J, that is the $m \times m$ matrix $\partial\mathbf{K}/\partial\mathbf{C}$ of these communities. The latter matrix determines the stability of the species-density subsystem on its own with the juvenile fraction of each species equal to its equilibrium value. More specifically, this reduced model of the species-density subsystem on its own is described by the same dynamic equations for the total species densities as in the full model (Eq. (13)), but with the fraction of juveniles Z_i in the populations taken constant over time and equal to the fraction of juveniles of the

species at equilibrium $\tilde{Z}_i$:

$$\frac{dC_i}{dt} = ((2-q)\gamma_i F_i - T_i)\,(1-\tilde{Z}_i)C_i - \mu_i C_i - \sum_{k>i} \alpha_k \psi_{ki} \frac{\left(\phi\tilde{Z}_i + (2-\phi)(1-\tilde{Z}_i)\right) C_i}{H_k + E_k} \left(q\tilde{Z}_k + (2-q)(1-\tilde{Z}_k)\right) C_k \quad [23]$$

Comparing the eigenvalues of this reduced model with the eigenvalues of the full model, in which the juvenile fraction in the population Z_i is dynamic and changes at the same time scale as the total species density, reveals the impact of dynamic changes in the population structure of the species on the stability of the community equilibrium. The eigenvalues of the reduced model can be computed from its Jacobian matrix which equals the matrix $\partial\mathbf{K}/\partial\mathbf{C} = \mathbf{V^1} + \mathbf{W^1}$. This matrix corresponds to the community matrix with elements $\partial(dC_i/dt)/\partial C_j$ that captures the per-capita effect of the species in the community on each other's growth rate and determines stability in community models without population structure.

To further assess the differences between constant and a dynamic juvenile fraction in the population, for all stable communities resulting from the stage-structured model with asymmetry in feeding and predation between juveniles and adults ($q = 0.7$, $\phi = 1.8$) community dynamics were computed starting from the equilibrium community state using the reduced model including the differential equations dC_i/dt for the species-density subsystem only (Eq. (23)), with the juvenile faction Z_i in each of the populations taken equal to its equilibrium value inferred from the stable community state (see Fig. 4C, top-left panel, in the main text and Fig. S6). Similarly, community dynamics were computed with an age-structured analogue of the full model. This age-structured model includes differential equations dC_i/dt for the species-density subsystem and dZ_i/dt for the species-structure subsystem, but substitutes the juvenile maturation rate $m_i(F_i)$ for each of the species in the community with a constant value. This constant value is equal to the maturation rate that juveniles of the species experience in the community equilibrium and is indicated with $\tilde{m}_i$. Dynamics are then described by the equations:

$$\frac{dC_i}{dt} = b_i(F_i)(1-Z_i)C_i - \mu_i C_i - (\phi Z_i + (2-\phi)(1-Z_i))\,C_i \sum_{k>i} \alpha_k \psi_{ki} \frac{(qZ_k + (2-q)(1-Z_k))\,C_k}{H_k + E_k} \quad [24]$$

$$\frac{dZ_i}{dt} = b_i(F_i)(1-Z_i)^2 - \tilde{m}_i Z_i - 2(\phi-1)(1-Z_i)Z_i \sum_{k>i} \alpha_k \psi_{ki} \frac{(qZ_k + (2-q)(1-Z_k))\,C_k}{H_k + E_k} \quad [25]$$

The simulations with this age-structured analogue were also started from the equilibrium community state (see Fig. 4C, top-right panel, in the main text and Fig. S6). For comparison, community dynamics were also computed with the full model including the differential equations dC_i/dt for the species-density subsystem (Eq. (3)) and dZ_i/dt for the species-structure subsystem (Eq. (4)) starting from a community state in which the initial density of each species was exactly 50% of its equilibrium value inferred from the stable community state (see Fig. 4C, bottom panel in the main text and Fig. S6).

Extent of self-regulation. For stable communities the extent of self-regulation of species is assessed with the diagonal elements of the community matrix, the $m \times m$ matrix $\partial\mathbf{K}/\partial\mathbf{C}$ (Eq. (17)), which measures the positive or negative effect of the total species abundance C_i on its own rate of change dC_i/dt (Fig. S5).

Stage-structured biomass model of species dynamics

To check the robustness of the results obtained with the stage-structured model in terms of juvenile and adult numerical densities, numerical simulations of community dynamics were also carried out, using a stage-structured biomass model for species dynamics (4). More specifically, each species was represented by 3 life history stages, referred to as juveniles, subadults and adults. Such a stage-structured biomass model (4) constitutes an approximation to a size-structured population model that accounts for a complete size distribution of individuals between their size at birth and size at maturation, in which the rates of feeding, metabolic maintenance, somatic growth, and reproduction all scale linearly with individual body size (5). Juvenile and subadult individuals are assumed to use their net-energy production (the difference between assimilation and metabolic maintenance rate) for somatic growth, whereas adults are assumed not to grow and use their net-energy production for reproduction. Dynamics are in terms of juvenile, subadult and adult biomass densities, indicated with J_i, S_i and A_i, respectively.

In the absence of predation the life history processes in the stage-structured biomass model are described by the following

mass-specific rate functions:

$$\text{Juvenile somatic growth} \quad g_i^J(F_i) = \max\left((2-q)\gamma_i F_i - T_i, 0\right) \quad [26]$$

$$\text{Subadult somatic growth} \quad g_i^S(F_i) = \max\left(q\gamma_i F_i - T_i, 0\right) \quad [27]$$

$$\text{Adult reproduction} \quad b_i(F_i) = \max\left((2-q)\gamma_i F_i - T_i, 0\right) \quad [28]$$

$$\text{Juvenile mortality} \quad d_i^J(F_i) = \mu_i - \min\left((2-q)\gamma_i F_i - T_i, 0\right) \quad [29]$$

$$\text{Subadult mortality} \quad d_i^S(F_i) = \mu_i - \min\left(q\gamma_i F_i - T_i, 0\right) \quad [30]$$

$$\text{Adult mortality} \quad d_i^A(F_i) = \mu_i - \min\left((2-q)\gamma_i F_i - T_i, 0\right) \quad [31]$$

$$\text{Juvenile maturation} \quad m_i^J(F_i) = \begin{cases} \dfrac{g_i^J(F_i) - D_i^J}{1 - z^{1-D_i^J/g_i^J(F_i)}} & \text{if } g_i^J(F_i) > 0 \\ 0 & \text{otherwise} \end{cases} \quad [32]$$

$$\text{Subadult maturation} \quad m_i^S(F_i) = \begin{cases} \dfrac{g_i^S(F_i) - D_i^S}{1 - z^{1-D_i^S/g_i^S(F_i)}} & \text{if } g_i^S(F_i) > 0 \\ 0 & \text{otherwise} \end{cases} \quad [33]$$

In these equations F_i represents the functional response of species i, which for the basal species equals:

$$F_1 = \frac{P}{\delta + \alpha_1\left((2-q)\,J_1 + q\,S_1 + (2-q)\,A_1\right)} \quad [34]$$

The parameter q in this expression determines the asymmetry in feeding capacity between juveniles, subadults and adults (for the purpose of this study taken the same for all species). Non-basal species forage following a type II functional response:

$$F_i = \frac{E_i}{H_i + E_i} \quad [35]$$

in which E_i represents the encounter rate of non-basal species i with prey biomass:

$$E_i = \sum_{k<i} \psi_{ik}\left(\phi\,J_k + (2-\phi)\,S_k + (2-\phi)\,A_k\right) \quad [36]$$

The parameter ϕ represents the bias of the consumer species toward feeding on juvenile as opposed to subadult and adult prey (for the purpose of this study taken the same for all species). Notice that all species are ordered according to their body size and hence species i can only feed on species with an index $k < i$.

The parameter T_i in the life history functions (26)-(33) represents the (mass-specific) loss rate through metabolic maintenance requirements, while the parameter μ_i represents the background mortality. The parameter γ_i determines the maximum assimilation rate per unit biomass, while the parameter z equals the ratio between the body size at entering and leaving each of the immature stages (the juvenile and subadult stage). The parameters γ_i, q and T_i also determine the minimum food availability that is needed by juveniles, subadults and adults to just keep itself alive without producing any offspring and without maturing.

D_i^J and D_i^S indicate the total mortality rate experienced by juvenile and subadult individuals, respectively, which in the absence of predation equals μ_i, but in the presence of predation also includes the predation mortality (see below; note that D_i^J and D_i^S do not include starvation mortality as starvation mortality only occurs when $g_i^J(F_i) = 0$ or $g_i^S(F_i) = 0$, in which case $m_i^J(F_i) = 0$ and $m_i^S(F_i) = 0$, respectively). Equations (28), (26), (27), (32) and (33) express that adult reproduction, juvenile and subadult growth in body size and juvenile and subadult maturation come to a halt under starvation conditions, which for juveniles, subadults and adults occur when $(2-q)\gamma_i F_i < T_i$, $q\gamma_i F_i < T_i$ and $(2-q)\gamma_i F_i < T_i$, respectively. Under these starvation conditions juveniles, subadults and adults experience increased mortality (Eqs. (29), (30) and (31)). The mass-specific juvenile and subadult maturation rates depends on both juvenile and subadult growth rate in body size as well as total juvenile and subadult mortality, D_i^J and D_i^S, respectively. The functional form of the maturation rates $m_i^J(F_i)$ and $m_i^S(F_i)$ is chosen such that any equilibrium state predicted by the stage-structured biomass model corresponds uniquely to an equilibrium state of a structured model that accounts for a complete size distribution of individuals between their size at birth and size at maturation, in which the rates of feeding, metabolic maintenance, somatic growth, and reproduction all scale linearly with individual body size (5).

A representation of each species by 3 life history stages with the smallest juveniles most vulnerable to predation mortality and the maturation of the larger immature individuals limited most by food availability was chosen because the dynamics of such a 3-stage biomass model has been found to closely resemble the dynamics of population models with a complete size distribution that are based on a dynamic energy budget model for the individual energetics (6). Similar results as presented in Fig. S7, S8 and S9 have, however, also been obtained using a stage-structured biomass model with only a single juvenile and adult life history stage to describe species dynamics.

The dynamics of the juvenile, subadult and adult biomass densities of all species in the community are now described by the following set of ordinary differential equations (ODEs):

$$\frac{dJ_i}{dt} = b_i(F_i)A_i + g_i^J(F_i)J_i - m_i^J(F_i)J_i - d_i^J(F_i)J_i - \phi J_i \sum_{k>i} \alpha_k \psi_{ki} \frac{(2-q)J_k + qS_k + (2-q)A_k}{H_k + E_k} \quad [37]$$

$$\frac{dS_i}{dt} = m_i^J(F_i)J_i + g_i^S(F_i)S_i - m_i^S(F_i)S_i - d_i^S(F_i)S_i - (2-\phi)S_i \sum_{k>i} \alpha_k \psi_{ki} \frac{(2-q)J_k + qS_k + (2-q)A_k}{H_k + E_k} \quad [38]$$

$$\frac{dA_i}{dt} = m_i^S(F_i)S_i - d_i^A(F_i)A_i - (2-\phi)A_i \sum_{k>i} \alpha_k \psi_{ki} \frac{(2-q)J_k + qS_k + (2-q)A_k}{H_k + E_k} \quad [39]$$

In these equations E_k and H_k represent the encounter rate with prey and the half-saturation density in the functional response of species k, respectively (Eq. (36)), while the parameters q and ϕ represent the asymmetry in foraging rate and predation risk, respectively, between juvenile, subadult and adult individuals. The default values for these parameters equal 1, implying that all 3 stages have identical life history rates ($q = 1$) and that consumers feed indiscriminately on juveniles, subadults and adults of their prey species ($\phi = 1$). Finally, the parameter α_k represents the maximum (mass-specific) foraging rate of consumer species k.

Given the above equations, the total juvenile mortality rate, on which the maturation rate (Eq. (32)) of juvenile into subadult biomass depends, is the sum of background (but not starvation) mortality and predation mortality:

$$D_i^J = \mu_i + \phi \sum_{k>i} \alpha_k \psi_{ki} \frac{(2-q)J_k + qS_k + (2-q)A_k}{H_k + E_k} \quad [40]$$

Starvation mortality is excluded from D_i^J because the maturation rate equals 0 under starvation conditions. Analogously, the total subadult mortality rate, on which the maturation rate (Eq. (33)) of subadult into adult biomass depends, is the sum of background (but not starvation) mortality and predation mortality:

$$D_i^S = \mu_i + (2-\phi) \sum_{k>i} \alpha_k \psi_{ki} \frac{(2-q)J_k + qS_k + (2-q)A_k}{H_k + E_k} \quad [41]$$

Model parameterisation and numerical simulation details. Parameterisation of the stage-structured biomass model follows the same procedure as the stage-structured model in terms of juvenile and adult abundance (see Materials and Methods). In short, half-saturation prey densities H_i for non-basal species are sampled from a uniform distribution on the interval $[0.5, 2.5]$. The ratio between the smallest and the largest body size in each of the two immature life stages, z, that occurs in the maturation rates of the stage-structured biomass model (Eq. (32)) and (Eq. (33)), is for all species taken the same and equal to $z = 0.1$. Individuals are hence assumed to grow 2 orders of magnitude in body size between birth and maturation. The parameters α_i, γ_i, T_i and μ_i all represent (mass-specific) rates and are assumed to scale with $w_i^{-0.25}$ following the equations:

$$\alpha_i = \alpha_0 \left(1 + 2\sigma_\alpha \left(x_{i1} - \tfrac{1}{2}\right)\right) w_i^{-0.25} \quad [42]$$

$$\gamma_i = \gamma_0 \left(1 + 2\sigma_\gamma \left(x_{i2} - \tfrac{1}{2}\right)\right) w_i^{-0.25} \quad [43]$$

$$T_i = T_0 \left(1 + 2\sigma_T \left(x_{i3} - \tfrac{1}{2}\right)\right) w_i^{-0.25} \quad [44]$$

$$\mu_i = \mu_0 \left(1 + 2\sigma_\mu \left(x_{i4} - \tfrac{1}{2}\right)\right) w_i^{-0.25} \quad [45]$$

The default mean values of the species-specific parameters equal $\alpha_0 = 1.0$, $\gamma_0 = 0.6$, $T_0 = 0.1$ and $\mu_0 = 0.015$ (6), while the species-specific parameters α_i, γ_i, T_i and μ_i are randomly selected from a Bates distribution of degree 3 around these mean values. A Bates distribution is the continuous probability distribution of the mean, X, of 3 independent uniformly distributed random variables on the unit interval. Random values from this distribution range between 0 and 1 with mean value of 1/2 and are easily generated by taking the mean of 3 independent samplings from a uniform distribution on the unit interval $[0, 1]$. The quantities x_{ij} are independent realisations of the random variable X, while σ_α, σ_γ, σ_T and σ_μ represent the one-sided, relative width of the distributions of the species-specific parameters α_i, γ_i, T_i and μ_i, respectively, around the mean values $\alpha_0 = 1.0$, $\gamma_0 = 0.6$, $T_0 = 0.1$ and $\mu_0 = 0.015$. Default values for these relative widths equal 0.1, such that all species-specific parameters α_i, γ_i, T_i and μ_i range between 0.9 and 1.1 times their default mean value and follow hump-shaped distributions within these ranges. The productivity P and turn-over rate δ of the exclusive resource of the basal species are taken equal to 60 and 2.0, respectively, in all computations. The two remaining parameters, the foraging asymmetry parameter q and the predation asymmetry parameter ϕ, in the model are varied between the different computations to assess their effect on community dynamics.

As described in the Materials and Methods section food webs are generated by selecting $N = 500$ random niche values n_i uniformly from the interval $[0, 1]$ and associated with species body mass following $w_i = (w_{max})^{n_i}(w_{min})^{(1-n_i)}$. Subsequently, the network of feeding interactions between these $N = 500$ species is constructed by generating for each non-basal species the midpoint of its feeding niche c_i following the procedure and default values for the mean prey-predator body mass ratio

described in the Materials and Methods and Fig. S10. Numerical integrations of the food web with $N = 500$ species are carried out using an adaptive Runge-Kutta (Cash-Karp) method implemented in C. Relative and absolute tolerances during the integration equal $1.0 \cdot 10^{-7}$ and $1.0 \cdot 10^{-13}$, respectively. During the first 10^4 time units no species are removed from the community, even if they attain very low density. For $t > 10^4$ each species, whose total biomass density $J_i + S_i + A_i$ drops below 10^{-8}, is removed from the community. This persistence threshold ensures that the product of the relative tolerance (10^{-7}) and the lowest species density (10^{-8}) is larger than the machine precision (equal to $1.11 \cdot 10^{-16}$ according to the IEEE 754-2008 standard in case of double precision). During numerical computations mean and variance as well as the maximum and minimum value of the total species biomass $J_i + S_i + A_i$ are continuously monitored for all species. The values of these measured statistics are reset whenever the community structure changes as one or more species in the community go extinct. Numerical integrations are halted whenever the community structure has not changed for 10^6 time units and no change has occurred from one time unit to the next in the values of these statistics (mean, minimum, maximum and variance of total species density) for all species in the community.

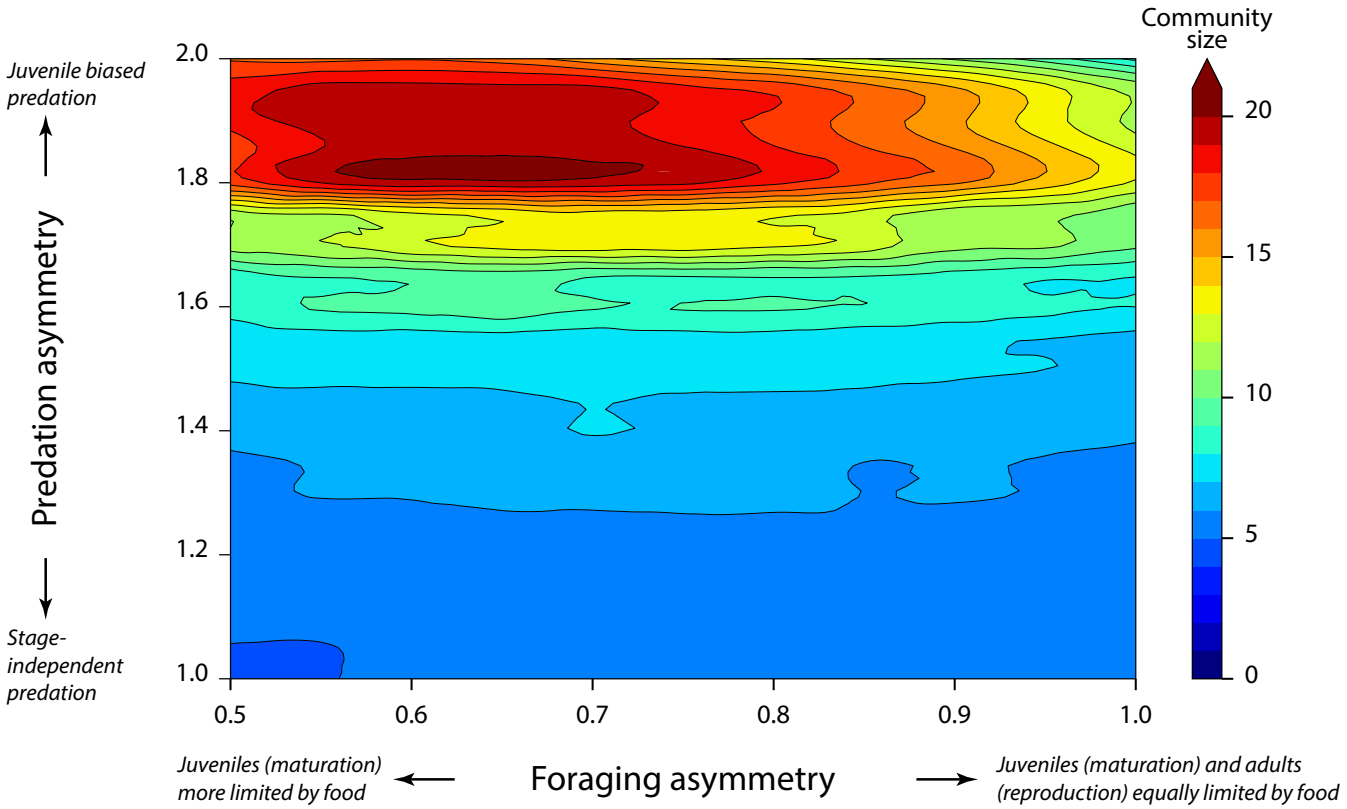

Fig. S1. Juvenile-adult asymmetry increases community diversity – Mean community size (non-basal species only) of 500 replicate food web simulations with juvenile-adult stage-structure for different values of foraging (q) and predation (ϕ) asymmetry between juveniles and adults. Larger communities result when predation is stronger on juveniles than on adults and maturation is more limited by food availability than reproduction.

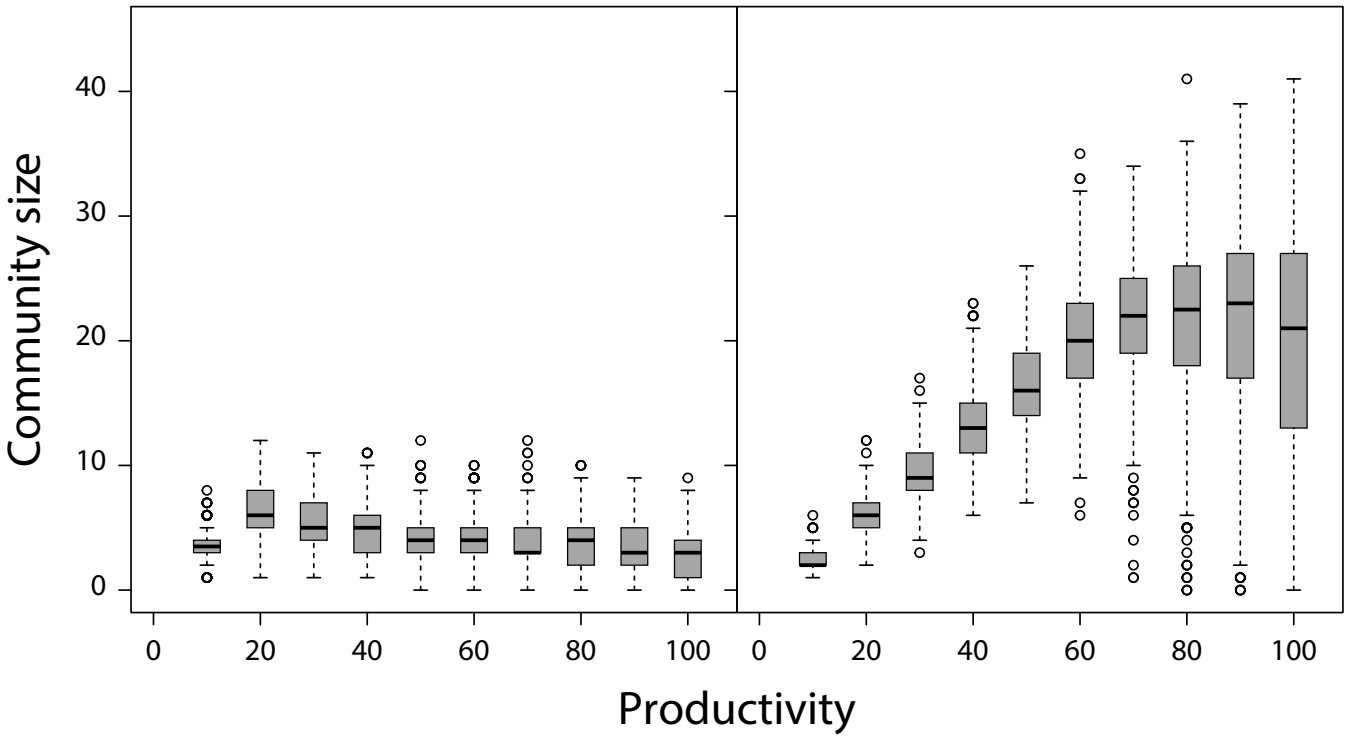

Fig. S2. Juvenile-adult asymmetry increases community diversity at all productivities – Boxplot of community sizes at different levels of system productivity P resulting from 500 replicate food web simulations without (*left*) and with stage-structure and foraging and predation asymmetry between juveniles and adults (*right*; $q = 0.7$, $\phi = 1.8$, see Materials and Methods).

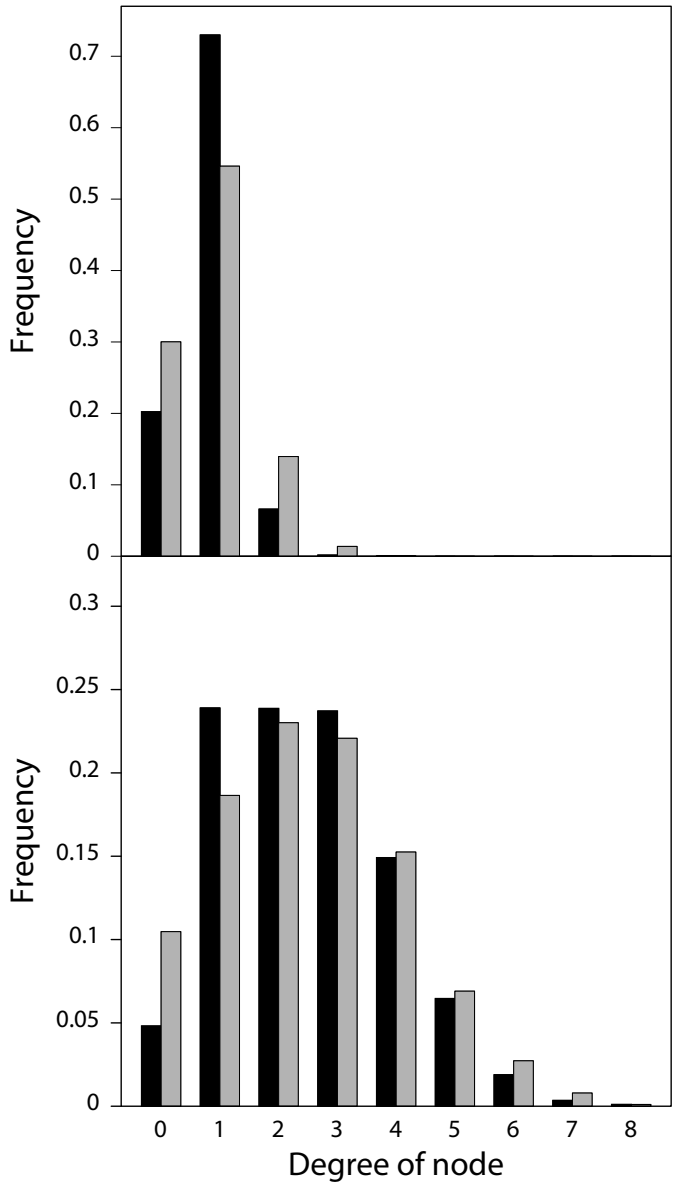

Fig. S3. Juvenile-adult asymmetry increases food web connectivity – Number of prey species (black bars; incoming network node links) and predators (grey bars; outgoing network node links) for all species in food webs resulting from 500 replicate simulations without (top panel) and with stage-structure and foraging and predation asymmetry between juveniles and adults (bottom panel; $q = 0.7$, $\phi = 1.8$).

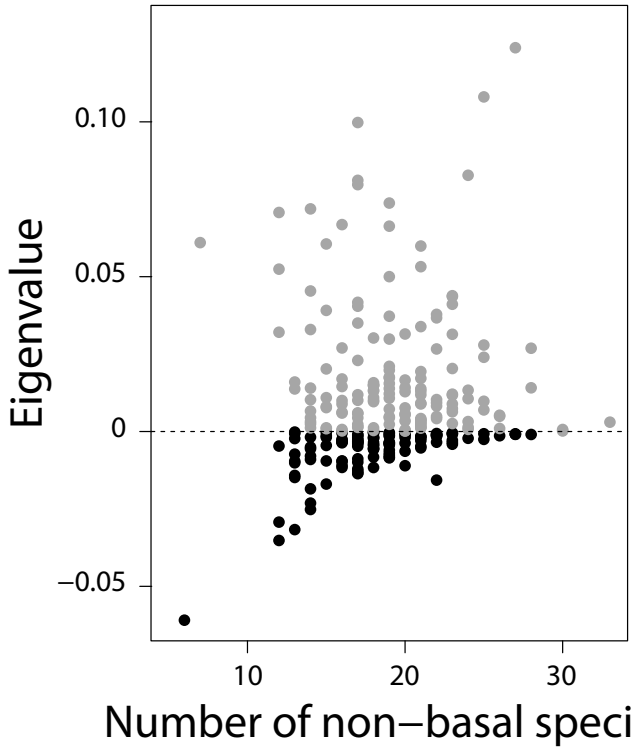

Fig. S4. Eigenvalues of the Jacobian matrix with largest real part determining community stability – Real part of the dominant (right-most) eigenvalue of the Jacobian matrix determining community stability as a function of community size for all stable communities (black dots) and all unstable communities for which the equilibrium could be solved for numerically (grey symbols) for the stage-structured model in case of foraging and predation asymmetry between juveniles and adults ($q = 0.7$, $\phi = 1.8$).

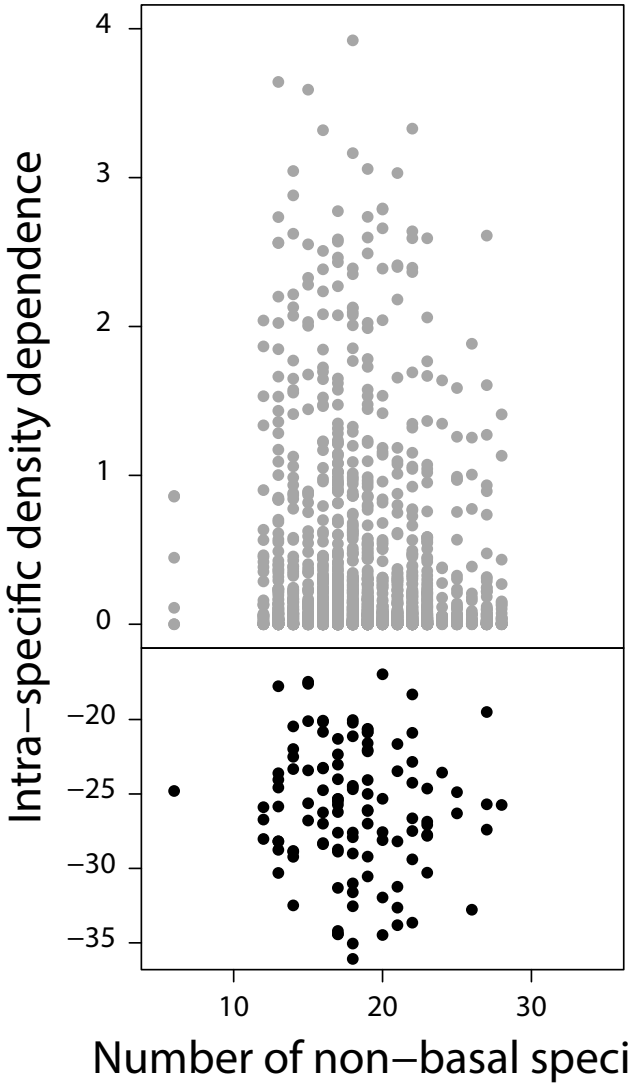

Fig. S5. Juvenile-adult asymmetry stabilises community dynamics without self-regulation – Strength of intra-specific density dependence for basal (*bottom*) and all non-basal species (*top*) in stable communities resulting from food web simulations with the stage-structured model and foraging and predation asymmetry between juveniles and adults ($q = 0.7, \phi = 1.8$). Intra-specific density dependence is assessed with the diagonal elements of the community matrix, which measures for basal and non-basal species the negative and positive effect, respectively, of total species abundance on its own rate of change (see Materials and Methods).

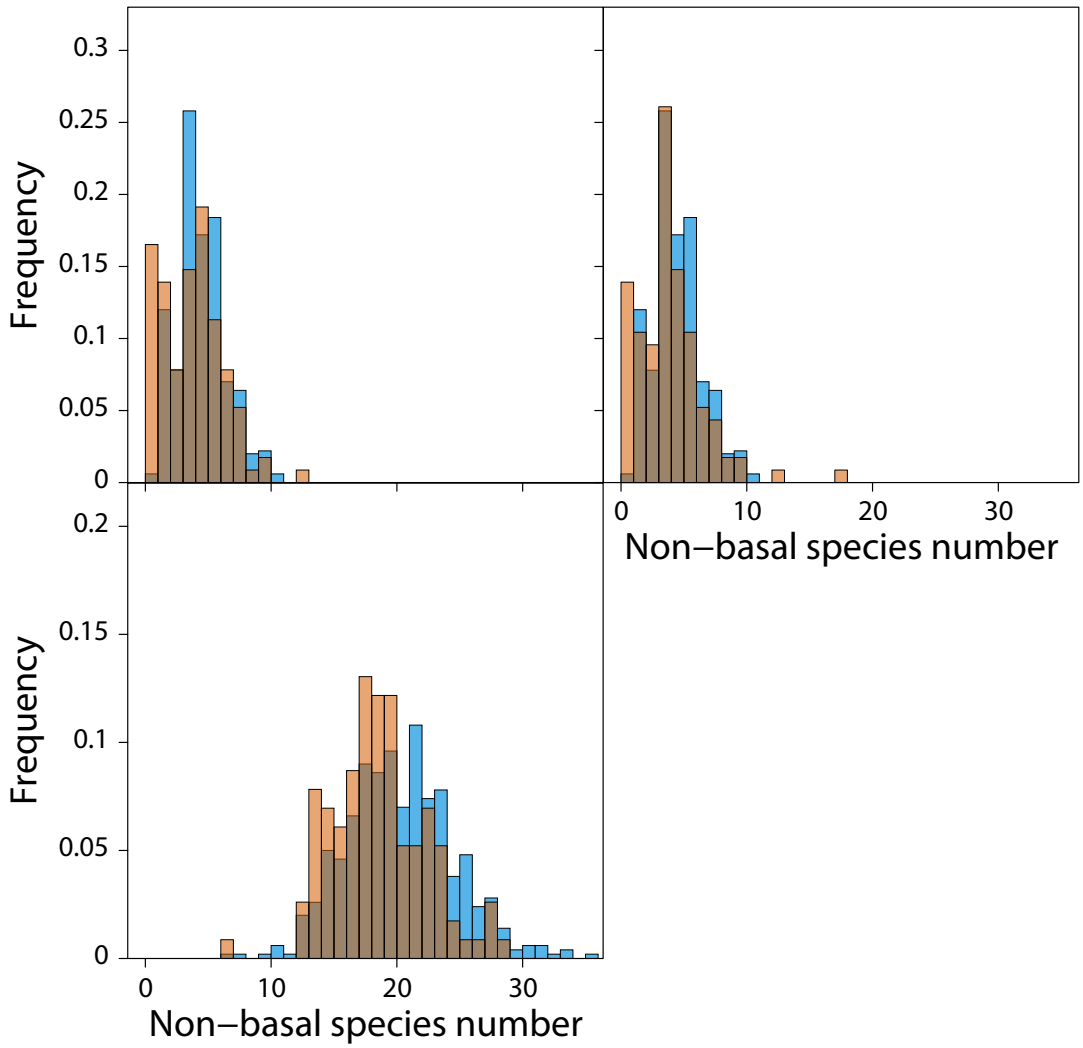

Fig. S6. Dynamic juvenile-adult ratio enforces complex community stability – Frequency distribution of community sizes (non-basal species only; red bars) resulting from simulations of dynamics for all stable communities generated by the stage-structured model in case of foraging and predation asymmetry between juveniles and adults ($q = 0.7$, $\phi = 1.8$) with different model variants (see Materials and Methods and section *Sources of community stability* above). Top-left panel shows results of the species-density subsystem on its own with the juvenile-adult ratio for each species constant in time and equal to its equilibrium value when initial species densities are identical to their equilibrium values. Top-right panel shows results of the coupled species-density and species-structure subsystem with the juvenile maturation rate for each species constant in time and equal to its equilibrium value when initial species densities are identical to their equilibrium values (These results represent dynamics of an analogous age-structured model). Bottom panel shows results of the coupled species-density and species-structure subsystem when initial densities for each species are reduced to 50% of their equilibrium densities. For reference, top and bottom panels also show the frequency distribution of community sizes (non-basal species only; blue bars) resulting from 500 replicate food web simulations without and with stage-structure and foraging and predation asymmetry between juveniles and adults, respectively, that are also presented in Figure 2 in the main text.

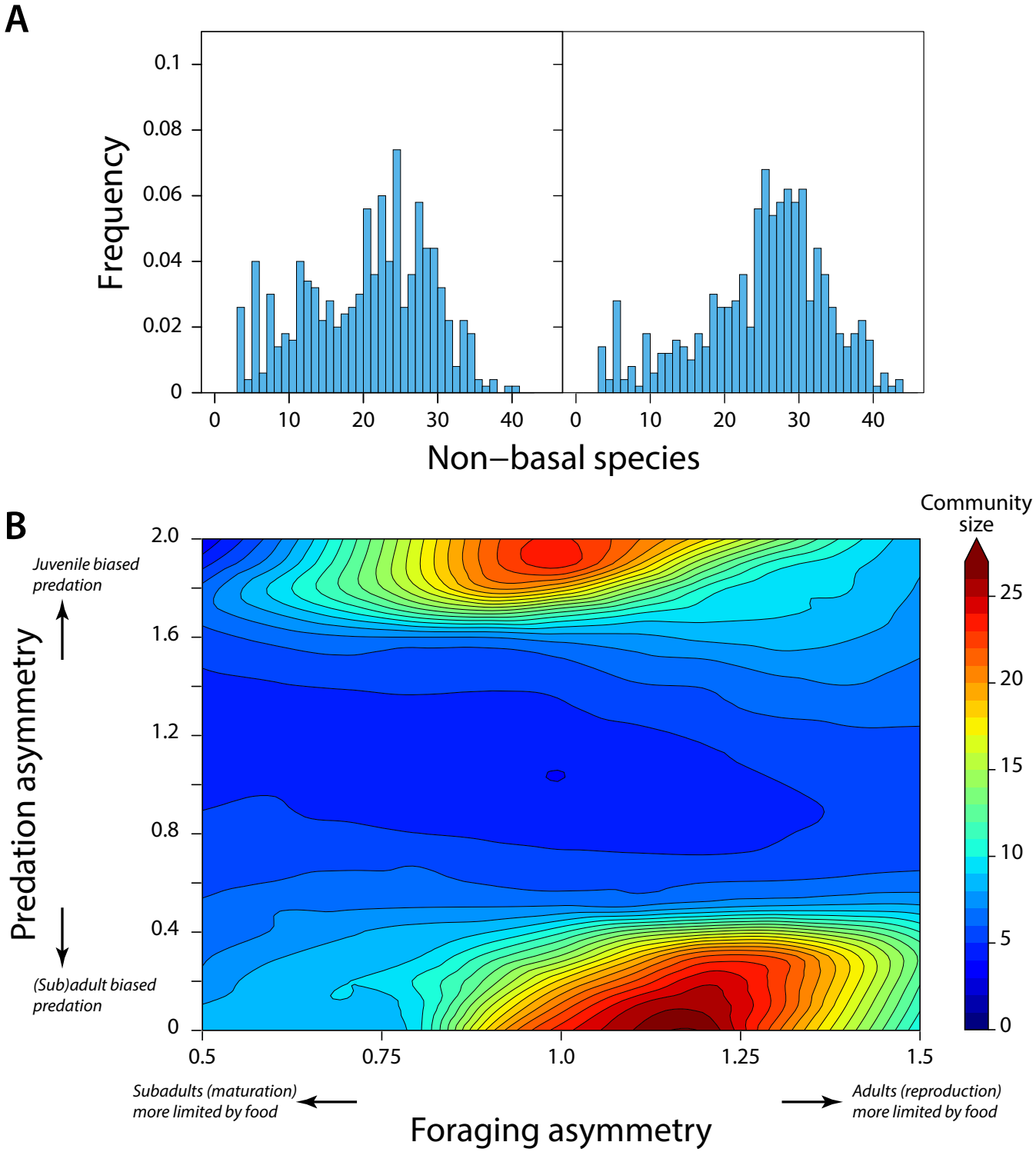

Fig. S7. Juvenile-adult asymmetry in biomass dynamics increases community diversity – *A*: Frequency distribution of community sizes (non-basal species only) resulting from 500 replicate food web simulations using the 3-stage biomass model including juveniles, subadults and adults (see section *Stage-structured biomass model of species dynamics* above) when juveniles are most vulnerable to predation and subadults are limited most by food availability (left panel; $q = 0.9$, $\phi = 1.8$) and when subadults and adults are more vulnerable to predation and small juveniles and adults are limited most by food availability (right panel; $q = 1.2$, $\phi = 0.2$). *B*: Mean community size (non-basal species only) of 500 replicate food web simulations using the 3-stage biomass model including juveniles, subadults and adults for different values of foraging (q) and predation (ϕ) asymmetry.

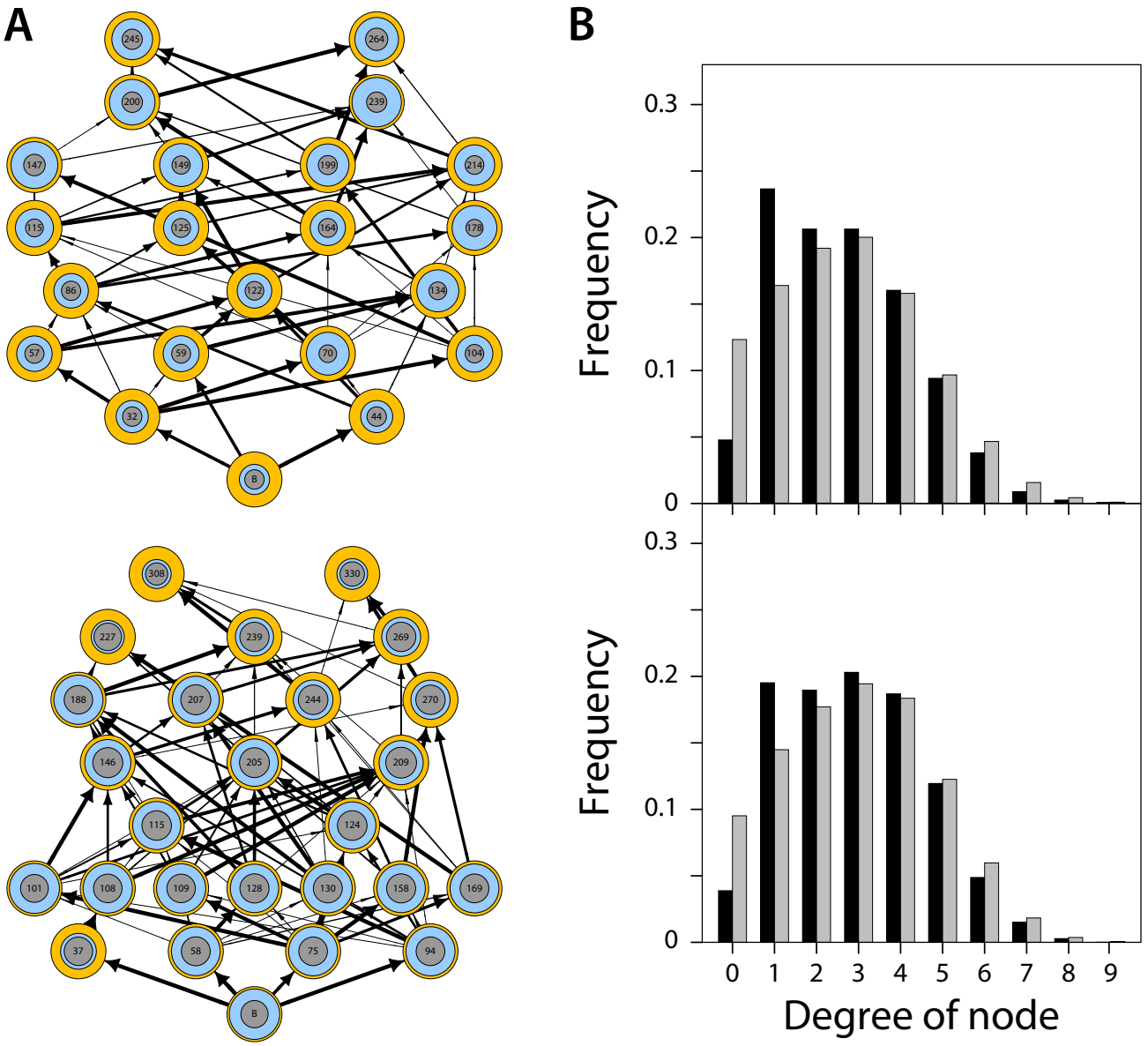

Fig. S8. Juvenile-adult asymmetry in biomass dynamics increases food web complexity – *A*: Examples of food webs resulting from simulations using the 3-stage biomass model including juveniles, subadults and adults (see *Stage-structured biomass model of species dynamics* above) when juveniles are more vulnerable to predation and subadults are limited most by food availability (top panel; $q = 0.9$, $\phi = 1.8$) and when subadults and adults are more vulnerable to predation and small juveniles and adults are limited most by food availability (bottom panel; $q = 1.2$, $\phi = 0.2$). Vertical position indicates trophic level. Inner circles indicate the biomass fraction of juveniles (grey) and total immatures (blue) in the population. Arrow widths indicate the relative feeding preference (ψ_{ik}, see Materials and Methods) of consumers for a particular prey species. *B*: Number of prey species (black bars; incoming network node links) and predators (grey bars; outgoing network node links) for all species in food webs resulting from 500 replicate simulations using the 3-stage biomass model including juveniles, subadults and adults when juveniles are more vulnerable to predation and subadults are limited most by food availability (top panel; $q = 0.9$, $\phi = 1.8$) and when subadults and adults are more vulnerable to predation and small juveniles and adults are limited most by food availability (bottom panel; $q = 1.2$, $\phi = 0.2$).

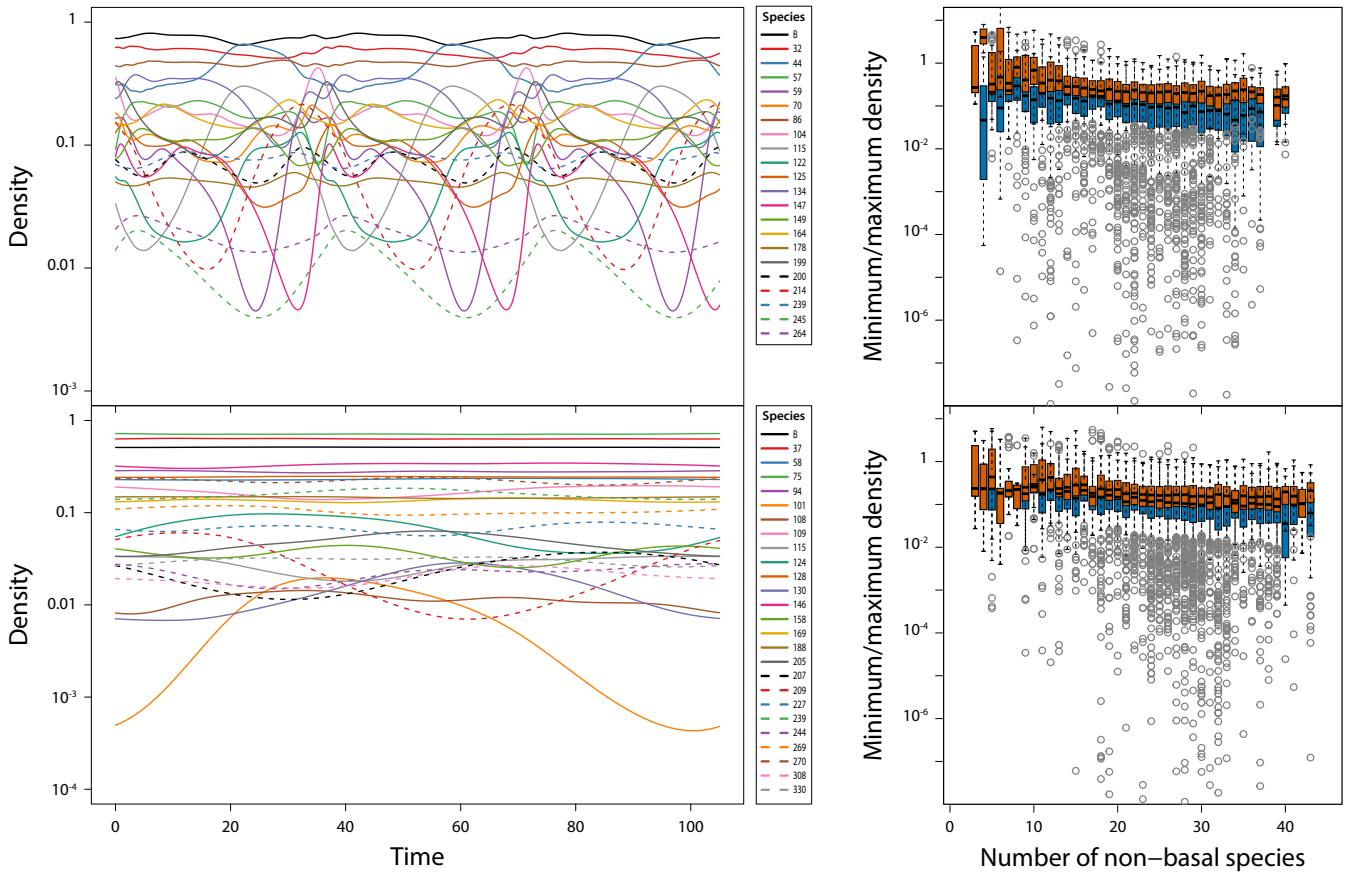

Fig. S9. Juvenile-adult asymmetry in biomass dynamics stabilises community dynamics – *A*: Examples of total biomass dynamics of all species in food web simulations using the 3-stage biomass model including juveniles, subadults and adults (see *Stage-structured biomass model of species dynamics* above) when juveniles are more vulnerable to predation and subadults are limited most by food availability (top panel; $q = 0.9$, $\phi = 1.8$) and when subadults and adults are more vulnerable to predation and juveniles are limited most by food availability (bottom panel; $q = 1.2$, $\phi = 0.2$). Corresponding food web structures are shown in Figure S8. *B*: Boxplot of minimum (blue bars) and maximum total biomass densities (red bars) as a function of community size for all persisting species in 500 replicate food web simulations using the 3-stage biomass model including juveniles, subadults and adults (see *Stage-structured biomass model of species dynamics* above) when juveniles are more vulnerable to predation and subadults are limited most by food availability (top panel; $q = 0.9$, $\phi = 1.8$) and when subadults and adults are more vulnerable to predation and small juveniles and adults are limited most by food availability (bottom panel; $q = 1.2$, $\phi = 0.2$).

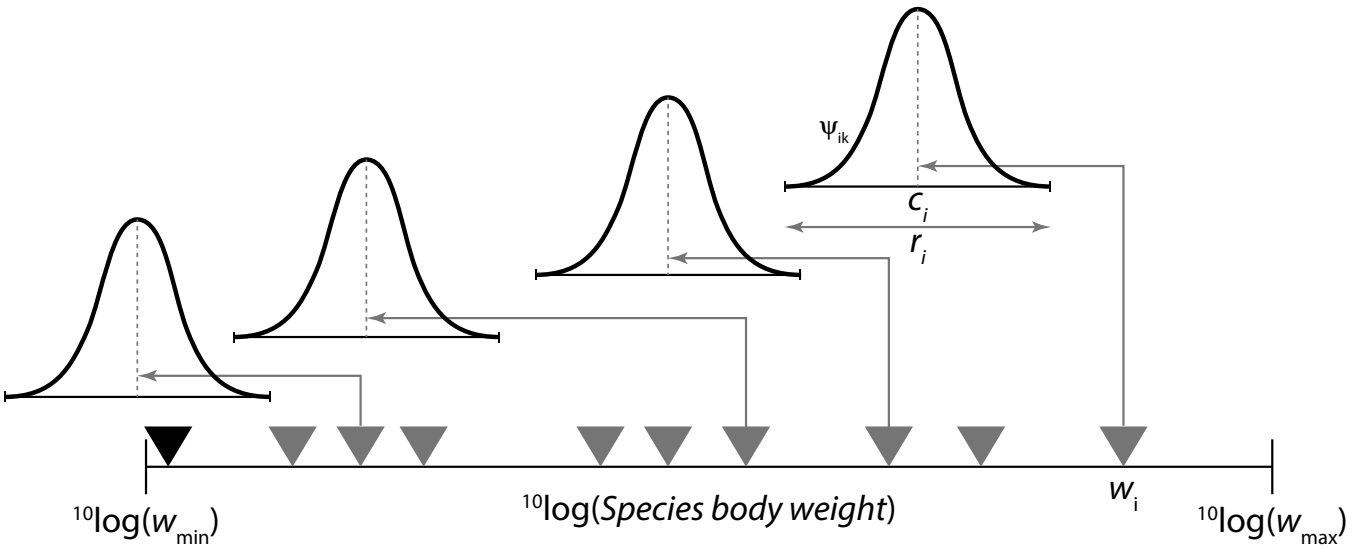

Fig. S10. Construction of the prey-predator mass ratio food web model – Species are randomly assigned niche values n_i in the range [0,1]. Niche values are related to body size w_i following $w_i = (w_{max})^{n_i}(w_{min})^{1-n_i}$ with minimum (w_{min}) and maximum body size (w_{max}) equal to 10^{-8} and 10^4 gram, respectively. The center c_i of the feeding niche of consumer species is uniformly distributed between $n_i - 2.5/^{10}\log(w_{max}/w_{min})$ and $n_i - 0.5/^{10}\log(w_{max}/w_{min})$, yielding median prey-predator body size ratio between $10^{-2.5}$ and $10^{-0.5}$. The feeding niche width r_i equals $1/^{10}\log(w_{max}/w_{min})$. Consumer species i feeds on all prey species k with body sizes between $(w_{max})^{(c_i-r_i/2)}(w_{min})^{(1-(c_i-r_i/2))}$ and $(w_{max})^{(c_i+r_i/2)}(w_{min})^{(1-(c_i+r_i/2))}$ at a relative feeding rate ψ_{ik} following a hump-shaped distribution of prey body size (see Materials and Methods).

References

1. Karline Soetaert. *rootSolve: Nonlinear root finding, equilibrium and steady-state analysis of ordinary differential equations*, 2009. R package 1.6.
2. Karline Soetaert and Peter M.J. Herman. *A Practical Guide to Ecological Modelling. Using R as a Simulation Platform.* Springer, Dordrecht, The Netherlands, 2009. ISBN 978-1-4020-8623-6.
3. R Core Team. *R: A language and environment for statistical computing.* R Foundation for Statistical Computing, Vienna, Austria, 2020.
4. A M de Roos, T Schellekens, T Van Kooten, K E Van De Wolfshaar, D Claessen, and L Persson. Food-dependent growth leads to overcompensation in stage-specific biomass when mortality increases: The influence of maturation versus reproduction regulation. *American Naturalist*, 170:E59–E76, 2007.
5. A M de Roos, T Schellekens, T Van Kooten, K E Van De Wolfshaar, D Claessen, and L Persson. Simplifying a physiologically structured population model to a stage-structured biomass model. *Theoretical Population Biology*, 73(1):47–62, 2008.
6. A M de Roos and L Persson. *Population and community ecology of ontogenetic development.* Monographs in Population Biology 51. Princeton University Press, Princeton, NJ, 2013.